35th Annual International Conference of the IEEE EMBS
Osaka, Japan, 3 - 7 July, 2013

Detection of Transient, Regional Cardiac Repolarization Alternans by Time-Frequency Analysis of Synthetic Electrograms

Michele Orini[1,3], Ben Hanson[2], Peter Taggart[1] and Pier Lambiase[1]

***Abstract*— Repolarization alternans (RA), originating at the cellular level, is thought to produce an arrhythmogenic substrate, and surface ECG T-wave alternans (TWA) is a marker of risk for sudden cardiac death. In this paper we study RA in the unipolar electrograms (EGM), which represent the electrical activity of the heart at the tissue level. We first describe a simple analytical model to study how RA, simulated as alternating variations of action potential duration, affects EGM-TWA, and then we propose a novel methodology based on time-frequency analysis to detect EGM-TWA which occurs intermittently in few consecutive beats. In a simulation study, we used a 257-node whole heart model to reproduce several patterns of RA. RA involved specific subsets of adjacent nodes (11, 65 and 257), exhibited different amplitudes (0.25, 0.5 and 1 ms) and lasted for 40 consecutive beats of a 80-beat-long test sequence. Results show a relationship between the spatial distribution of RA and EGM-TWA: the smaller the region where RA occurs, the higher the extent of EGM-TWA. With the proposed methodology, we localized those portions of myocardium which exhibited EGM-TWA with an accuracy higher than 90%.**

I. INTRODUCTION

Repolarization alternans (RA) is a multi-scale phenomenon that can produce an arrythmogenic substrate and is thought to be mechanicistically related to sudden cardiac death [1]. At the cellular level, RA occurs as an alternating pattern of consecutive action potential durations (APD) [2], while at the whole-organ level, RA gives rise to the so called ECG T-wave alternans [3].

Electrograms (EGM) recorded on the surface of the myocardium offer the opportunity to study the electrical activity of the heart at the tissue level. EGM incorporate features from both the transmembrane potential, providing indirect estimates of local depolarization and repolarization times [4], and the ECG, exhibiting a similar waveform which also includes a T-wave. Therefore, EGM can help to clarify how RA originating at the cellular level is represented in the surface ECG, which is widely used for non-invasive diagnosis. This would help to understand the role of RA in arrhythmogenesis and to achieve more accurate predictions of arrhythmic risk. Moreover, thanks to advances in cardiac catherization and the use of implantable cardiac defibrillators, EGM data are becoming more easily available. In this context, the design of accurate techniques for the quantification of RA in the EGM becomes very important. However, few methodological studies have been undertaken with this objective [5], [6].

The focus of this study is to examine the relationship between the spatial organization of APD alternans and the EGM T-wave alternans (EGM-TWA). We first try to understand how the size of the region affected by APD alternans affects the morphology of the EGM T-wave. To this end, we use a simple analytical model [7] to generate real-like unipolar EGM from synthetic action potentials [8], and simulate regional RA by modifying the APD locally. We then suppose that RA is a transient phenomenon, i.e. that it may occur in short period of time. In such a situation, traditional techniques based on spectral analysis are not appropriate and may not be able to correctly detect EGM-TWA. To overcome this issue, we propose and validate a methodology based on time-frequency analysis [9].

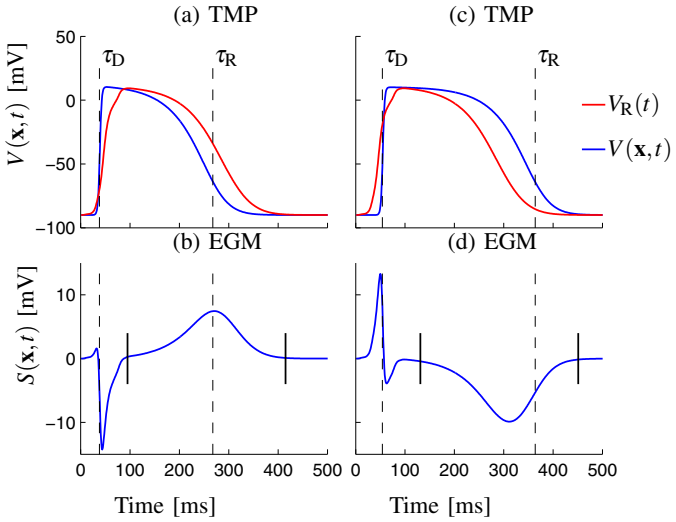

Fig. 1. Upper panels: Transmembrane potentials, $V(\mathbf{x},t)$, and remote component, $V_R(t)$ for 2 nodes. τ_D and τ_R are depolarization and repolarization times as in (1). (a)-(b) TMP with short τ_R corresponds to a positive T-wave; (c)-(d) TMP with long τ_R corresponds to a negative T-wave; Solid vertical lines represent the window for the T-wave, $[t_{ref} : t_{ref} + 320]$ ms.

II. SYNTHESIS OF UNIPOLAR ELECTROGRAMS

A. Synthetic EGM from analytical transmebrane potentials

1) Analytical transmebrane potentials: The transmembrane potentials of N=257 sources (*nodes*), each one localized at a given point $\mathbf{x}$ on the epi- end endocardium, were generated by using the analytical expression proposed in [8],

*This work was supported by the UK Medical Research Council (G0901819)

[1] M. Orini, P. Taggart and P. Lambiase are with the Institue of Cardiovascular Science, University College London, UK. m.orini@ucl.ac.uk, peter.taggart@uclh.nhs.uk, pier.lambiase@uclh.nhs.uk

[2] B. Hanson is with the Department of Mechanical Engineering, University College London, London, UK. b.hanson@ucl.ac.uk

[3] M. Orini is also with the CIBER-BBN, Zaragoza, Spain.

and already used for similar purposes in [10]:

$$V(\mathbf{x},t) = a(\mathbf{x})D(\mathbf{x},t)R(\mathbf{x},t) - V_0 \quad (1)$$

where for each $\mathbf{x}$, depolarization and repolarization phases are described by [8]:

$$D(t) = \frac{1}{1+e^{-\beta_{\mathrm{D}}(t-\tau_{\mathrm{D}})}} \quad (2)$$

$$R(t) = \left(1 - \frac{1}{1+e^{-\beta_{\mathrm{R1}}(t-\tau_{\mathrm{R}})}}\right)\left(1 - \frac{1}{1+e^{-\beta_{\mathrm{R2}}(t-\tau_{\mathrm{R}})}}\right) \quad (3)$$

In these expressions, τ_{D} and τ_{R} are the depolarization and repolarization times; β_{D}, β_{R1} and β_{R2} describe the upstroke during depolarization, and the leading and trailing downslope during repolarization, respectively; $a(\mathbf{x})$ is the amplitude of the transmembrane potential and V_0 is the resting potential. The action potential duration (APD) is defined as $\tau_{\mathrm{R}} - \tau_{\mathrm{D}}$. The values of the parameters were obtained by fitting $V(\mathbf{x},t)$ with the transmembrane potential of each node provided by ECGSIM [11] for a normal male. In the following, RA is simulated by modifying τ_{R}.

2) Synthetic unipolar electrograms: EGM characterized by a controlled RA pattern were generated by using the simple model proposed and validated in [7]. This simple model is derived from the bidomain model [12], assuming that the conductances of the myocardium are isotropic and homogeneous. EGM are estimated as the weighted difference between an inverted action potential and a remote component $V_{\mathrm{R}}(t)$, obtained by averaging $V(\mathbf{x},t)$ over all nodes $\mathbf{x}$:

$$S(\mathbf{x},t) = -\frac{g_i}{g_i+g_e}\big(V(\mathbf{x},t) - V_{\mathrm{R}}(t)\big) \quad (4)$$

where g_i and g_e are the conductances of intra- and extracellular domain, respectively, and $g_i/(g_i+g_e) = 0.25$ [7]. An example of $V(\mathbf{x},t)$, $V_{\mathrm{R}}(t)$ and $S(\mathbf{x},t)$ is given in Fig. 1.

B. Regional transient repolarization alternans

Unipolar EGM characterized by controlled patterns of repolarization alternans are simulated as follows: (i) A sequence of repolarization times, $\{\tau_{\mathrm{R,k}}^{(\mathbf{x})}\}$, is defined for any node $\mathbf{x}$ and heart beat $k = \{1 : N_{\mathrm{b}} = 80\}$. (ii) For each one of the N nodes, a sequence of N_{b} EGM, $S_{\mathrm{k}}(\mathbf{x},t)$, is generated by using (1)–(4) with $t \in (0,T)$, where T is a constant heart period. (iii) A signal representing the EGM recorded at $\mathbf{x}$ is created by concatenating several heart beats and adding a noise term:

$$y(\mathbf{x},t) = [S_1(\mathbf{x},t),\ldots,S_{\mathrm{k}}(\mathbf{x},t),\ldots,S_{\mathrm{N}_b}(\mathbf{x},t)] + \xi(\mathbf{x},t) \quad (5)$$

where $\xi(\mathbf{x},t)$ accounts for disturbances and artifacts.
In baseline conditions, repolarization times are random variables following a Normal distribution:

$$\left\{\tau_{\mathrm{R,k}}^{(\mathbf{x})}\right\} \sim \mathscr{N}\left(\tau_{\mathrm{R},0}^{(\mathbf{x})}, \sigma^2\right), \ \forall \mathbf{x} \text{ and } k \in \{1 : N_{\mathrm{b}} = 80\} \quad (6)$$

where $\tau_{\mathrm{R},0}^{(\mathbf{x})}$ are the repolarization times estimated by fitting $V(\mathbf{x},t)$ with the transmembrane potential provided by ECGSIM. The variation of $\{\tau_{\mathrm{R,k}}^{(\mathbf{x})}\}$ is small compared to baseline repolarization times ($\sigma << \tau_{\mathrm{R},0}^{(\mathbf{x})}$), and is intended to create more physiological patterns in which alternation may be generated by chance even in absence of RA. RA is simulated by modifying $\{\tau_{\mathrm{R,k}}^{(\mathbf{x})}\}$ as:

$$\left\{\tau_{\mathrm{R,k}}^{(\mathbf{x})}\right\} \sim \tau_{\mathrm{R},0}^{(\mathbf{x})} + A_{\mathrm{k}}\left(-\frac{1}{2}\right)^{\mathrm{k}}, \ k \in T_{\mathrm{RA}}, \ \mathbf{x} \in \Omega \quad (7)$$

where A_{k} is a random sequence from an uniform distribution with mean and variance equal to $\mathscr{U} \sim (A_{\mathrm{M}}, (0.25A_{\mathrm{M}})^2)$, which modulates the amplitude of the RA pattern; $T_{\mathrm{RA}} \in \{21 : 60\}$ are the heart beats affected by RA, and Ω indicates the subset of adjacent nodes affected by RA. Thus, RA is simulated as transient, regional, and with a stochastic amplitude: it lasts for 40 consecutive beats of the 80-beat-long test sequence and involves a specific subsets of nodes.

III. TIME-FREQUENCY ANALYSIS OF REPOLARIZATION ALTERNANS

This technique based on time-frequency analysis is an improved extension of the traditional spectral method [5], [3], designed to estimate RA continuously, rather than provide one average measure of RA over a certain period of time. For any node $\mathbf{x}$, the procedure is composed of the following steps:

(1) $y(t)$ is low-pass filtered with a cut-off frequency equal to 25 Hz.
(2) The filtered signal is reorganized in a matrix $\mathbf{Y} = [\mathbf{y}_1,\ldots,\mathbf{y}_{\mathrm{k}},\ldots,\mathbf{y}_{\mathrm{N}_b}]$. Each column of $\mathbf{Y}$, $\mathbf{y}_{\mathrm{k}}$, is the k-th T-wave, evaluated for $t \in [t_{\mathrm{ref}} : t_{\mathrm{ref}} + 320]$ ms, being $t_{\mathrm{ref}} = \tau_{\mathrm{D}} + \frac{1}{4N_b}\sum_k(\tau_{\mathrm{R,k}} - \tau_{\mathrm{D}})$.
(3) Columns of $\mathbf{Y}$ are downsampled with a downsampling factor equal to $\Delta T = 16$ to reduce the number of time-frequency distributions to be estimated. Rows of $\mathbf{Y}$ are detrended using a filter which computes the differences between each column, i.e. performing $\mathbf{y}_{\mathrm{k}} - \mathbf{y}_{\mathrm{k}-1}$, and then upsampled with an upsampling factor equal to 2 to prevent border effect in the time-frequency distribution. The rows of the new matrix, $\mathbf{Y}^{\mathrm{D}}$, represent the beat-to-beat variation of the T-wave, evaluated at any ΔT.
(4) Multitaper reassigned spectrograms (MTRS) [9] are estimated for any row of $\mathbf{Y}^{\mathrm{D}}$, and then averaged to obtain an aggregate distribution, $P(k,f)$. Any MTRS is obtained as follows: M spectrograms are estimated by using M orthogonal Hermite functions; The reassignment technique is used to enhance the time-frequency localization; The M reassigned spectrograms are averaged to reduce the variability of the reassignment process [9].
(5) The K-score [3], [5] is estimated as:

$$\mathscr{K}(k) = \frac{P_{\mathrm{RA}}(k) - P_{\mathrm{N}}(k)}{\sigma_{\mathrm{N}}(k)} \quad (8)$$

where $P_{\mathrm{RA}}(k)$ is the spectral peak of the RA oscillation, evaluated as the maximum of $P(k,f)$ for $f \in [0.495, 0.505]$ cycles/beats, $P_{\mathrm{N}}(k)$ and $\sigma_{\mathrm{N}}(k)$ are the mean and the standard deviation of $P(k,f)$ estimated in the noise spectral band [0.3,0.46] cycles/beats.

(6) RA is detected whenever $\mathscr{K}(k) > 3$ for at least L_{Th} consecutive beats.

IV. SIMULATION STUDY

Nine different conditions were simulated: RA can be global, $\Omega = \Omega_{\mathrm{G}}$ involves all the nodes; Regional, for $\Omega = \Omega_{\mathrm{R}}$, in which RA appears in the 64 closest nodes to a given one chosen randomly; Local, for $\Omega = \Omega_{\mathrm{L}}$, in which RA appears in the 10 closest nodes to a given one chosen randomly. For each of these three spatial patterns of activity, three amplitudes of RA were simulated, $A_{\mathrm{M}} = \{0.25, 0.5, 1\}$ ms. The standard deviation of $\{\tau^{(\mathbf{x})}_{\mathrm{R,k}}\}$ outside T_{RA} was $\sigma = 0.25 A_{\mathrm{M}}$. Each one of these 9 conditions was repeated 50 times, and at each iteration Ω, A_{k}, $\{\tau^{(\mathbf{x})}_{\mathrm{R,k}}\}$ changes consequently. The white Gaussian noise, $\xi(t)$ in (5), was set to give a SNR=40 dB and $T = 600$ ms. MTRS were estimated using 512 frequency points and $M = 3$ Hermite functions. The first Hermite function gave a spectrogram characterized by time and frequency resolution of 2.5 beats and 0.18 cycle/beats, respectively. MTRS technique largely improves this resolution.

V. RESULTS

Using the proposed model, we were able to generate EGM with T-waves exhibiting the wide range of different morphologies usually observed in real clinical recordings. As shown in Fig 1, positive T-waves were associated to nodes which repolarize earlier, while negative T-waves corresponded to nodes which repolarize later. At baseline heart beat, the proportion of positive, negative and bipolar T-waves was about 51%, 28% and 21%, respectively.

Figure 2 and 3 show that the amplitude of the EGM-TWA, i.e. the extent of the beat-to-beat changes in the morphology of the T-wave, depended on both the extent of APD alternans and the spatial organization of RA. Figure 2 illustrates the mean of the even and odd T-waves, estimated during T_{RA}, for any condition. An increase in the extent of APD alternans, A_{M}, causes an increase in the difference between even and odd T-waves. Interestingly, Fig. 2 also shows that the smaller the region affected by RA, Ω, the greater EGM-TWA. The dependence of the extent of EGM-TWA on both A_{M} and Ω is shown in Fig. 3, where EGM-TWA is quantified for each iteration, $\mathbf{x} \in \Omega$ and $k \in T_{\mathrm{RA}}$, as the ratio between the maximum of the difference between even and odd T-waves (in $S_{\mathrm{k}}(\mathbf{x},t)$), and the maximum of the average T-wave. When the size of the region affected by RA decreased, the extent of EGM-TWA increased. This figure also shows that the simulated extent of EGM-TWA was very low, going from 0.3/0.1%, for Ω_{G} and $A_{\mathrm{M}} = 0.25$ms, to 6.5/6.5%, for Ω_{L} and $A_{\mathrm{M}} = 1$ms (median/interquartile range).

The accuracy in the spatial localization of EGM-TWA is shown in Fig. 4. Accuracy was estimated as the mean of $(TP+TN)/(TP+FP+TN+FN)$ over 50 iterations, where TP and TN are true positive and negative detections, and FP and FN are false positive and negative detections (TP is the number of nodes for which $\mathscr{K}(k) > 3$ for at least L_{Th} consecutive beats). Figure 4 shows that when $L_{\mathrm{Th}} \geq 14$ beats,

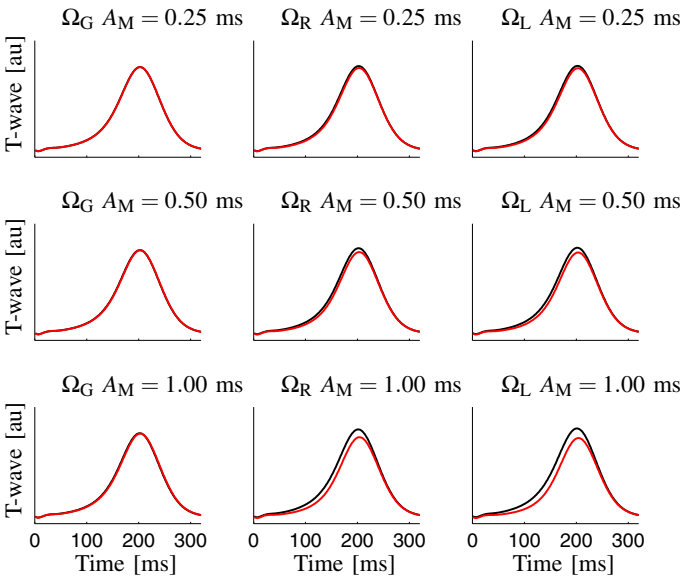

Fig. 2. Extent of EGM-TWA depending on the amplitude and spatial organization of RA. Mean T-waves in even and odd beats are reported in black and red, respectively. Amplitude of APD alternans was $A_{\mathrm{M}} = \{0.25, 0.5, 1\}$ ms, while global, regional and local RA affects $\{\Omega_{\mathrm{G}}, \Omega_{\mathrm{R}}, \Omega_{\mathrm{L}}\} = \{257, 65, 11\}$ nodes, respectively.

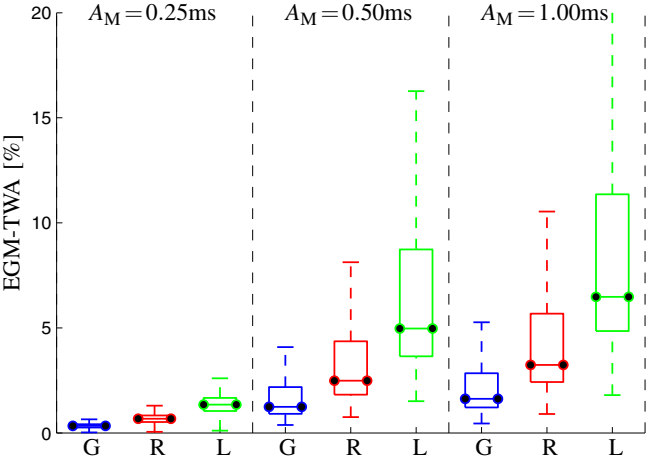

Fig. 3. Extent of EGM-TWA normalized over the amplitude of the average T-wave. Amplitude of APD alternans was $A_{\mathrm{M}} = \{0.25, 0.5, 1\}$ ms, while global, regional and local RA affects $\{\Omega_{\mathrm{G}}, \Omega_{\mathrm{R}}, \Omega_{\mathrm{L}}\} = \{257, 65, 11\}$ nodes, respectively.

for Ω_{R} and Ω_{L} accuracy was $\geq 94\%$ and $\geq 99\%$, repsectively, for all A_{M}. For Ω_{G}, better accuracy was achieved for shorter L_{Th}. In this case, for $L_{\mathrm{Th}} = 6$ beats, detection rate was 68% and 88% for $A_{\mathrm{M}} = 0.25$ and $A_{\mathrm{M}} = 1$ms, respectively. This shows that when RA is localized in a small region of the myocardium, EGM-TWA can be detected accurately even for small RA amplitude. Globally, these results show that by using the proposed methodology, we could correctly detect transient not-visible EGM-TWA with high accuracy.

VI. DISCUSSION

The main contributions of this study are: (i) We proposed a framework to simulate real-like patterns of EGM-

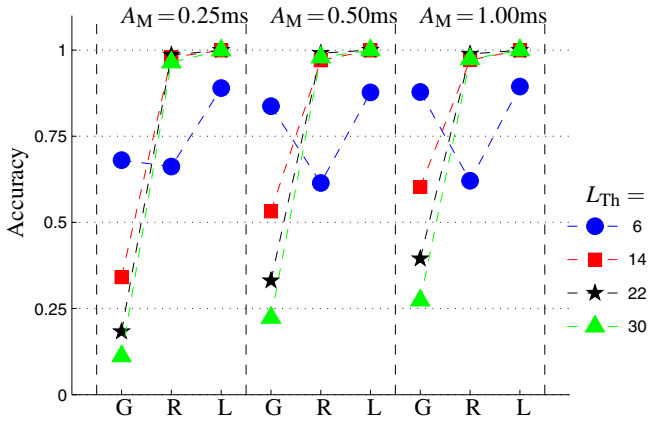

Fig. 4. Accuracy (average over 50 realizations) in the detection and localization of EGM-TWA. A_M is the amplitude of the APD alternans, and G, R and L represent global, regional and local RA. In a given node, EGM-TWA is detected when KS-score > 3 for at least L_{Th} consecutive beats.

TWA, by modifying the repolarization times of analytical transmembrane potential functions [8], which are then used to generate EGM waveforms [7]. (ii) We propose a novel methodology to detect EGM-TWA based on MTRS [9]. (iii) We use the proposed framework to investigate how the spatial distribution of RA at cellular level affects the EGM T-wave morphology, and to assess whether the proposed methodology can be used to correctly identify EGM-TWA which occurs in short periods of time.

Our results show that there is a relationship between the spatial distribution of RA at the cellular level and the extent of EGM-TWA: the smaller the region affected by RA, the higher the extent of EGM-TWA. This can be explained by the model in (4), since it can be shown that when the morphology of the transmembrane potential changes in few nodes, the remote component $V_R(t)$ remains almost unchanged, and this increases, in presence of RA, the difference between local and remote components, which is proportional to the local EGM. If the relationship between the degree of regionality of RA and the extent of EGM-TWA is confirmed in real data, it would support the strength of EGM-TWA as a predictor of sudden cardiac death, since it is thought that spatial gradients of repolarization may be associated with vulnerability to ventricular arrhythmias [1].

Our results also show that the proposed scheme based on MTRS can be used to detect EGM-TWA accurately, even when it is not-visible and lasts for few beats. The MTRS combines the reassignment, which enhances time-frequency localization, with multitapering, which reduces variability, and it is therefore an appropriate tool for TWA analysis [9]. However, comparisons with other methodologies are needed. Further studies should also include the characterization of more complex gradient of RA, which takes into account discordant RA, and the investigation of the relationship between EGM and surface ECG.

VII. CONCLUSIONS

In this paper, we used an analytical model to study how repolarization alternans, simulated at cellular level as alternating variations of APD, affects EGM-TWA, and we proposed a novel methodology based on time-frequency analysis to detect EGM-TWA even when it occurs in only a few beats. The results show that the smaller the region which exhibits APD alternans, the more apparent the extent of TWA on electrogram (EGM) recordings. This suggests that EGM-TWA can depend on the spatial gradients of repolarization, and is therefore an important tool in TWA measurement and analysis. We also show that the proposed time-frequency technique can accurately localize regions characterized by EGM-TWA, even when it occurs in a few beats.

VIII. ACKNOWLEDGMENTS

Michele Orini would like to thank Prof. Roberto Sassi for valuable comments and making available useful data.

REFERENCES

[1] J. M. Pastore, S. D. Girouard, K. R. Laurita, F. G. Akar, and D. S. Rosenbaum, "Mechanism linking T-wave alternans to the genesis of cardiac fibrillation." *Circulation*, vol. 99, no. 10, pp. 1385–1394, Mar 1999.

[2] J. Weiss, M. Nivala, A. Garfinkel, and Z. Qu, "Alternans and arrhythmias : From cell to heart," *Circulation Research*, vol. 108, no. 1, pp. 98–112, 2011.

[3] R. Verrier, T. Klingenheben, M. Malik, N. El-Sherif, D. Exner, S. Hohnloser, T. Ikeda, J. Martinez, S. Narayan, T. Nieminen, and D. Rosenbaum, "Microvolt T-wave alternans: Physiological basis, methods of measurement, and clinical utilityconsensus guideline by international society for holter and noninvasive electrocardiology," *Journal of the American College of Cardiology*, vol. 58, no. 13, pp. 1309–1324, 2011.

[4] B. Hanson, J. Gill, D. Western, M. P. Gilbey, J. Bostock, M. R. Boyett, H. Zhang, R. Coronel, and P. Taggart, "Cyclical modulation of human ventricular repolarization by respiration." *Front Physiol*, vol. 3, p. 379, 2012.

[5] D. Christini, K. Stein, S. Hao, S. Markowitz, S. Mittal, D. Slotwiner, S. Iwai, M. Das, and B. Lerman, "Endocardial detection of repolarization alternans." *IEEE transactions on bio-medical engineering*, vol. 50, no. 7, pp. 855–862, 2003.

[6] R. Selvaraj, P. Picton, K. Nanthakumar, S. Mak, and V. Chauhan, "Endocardial and epicardial repolarization alternans in human cardiomyopathy. Evidence for spatiotemporal heterogeneity and correlation with body surface T-wave alternans," *Journal of the American College of Cardiology*, vol. 49, no. 3, pp. 338–346, 2007.

[7] M. Potse, A. Vinet, T. Opthof, and R. Coronel, "Validation of a simple model for the morphology of the t wave in unipolar electrograms." *Am J Physiol Heart Circ Physiol*, vol. 297, no. 2, pp. H792–H801, Aug 2009.

[8] P. van Dam, T. Oostendorp, A. Linnenbank, and A. van Oosterom, "Non-invasive imaging of cardiac activation and recovery," *Annals of Biomedical Engineering*, vol. 37, no. 9, pp. 1739–1756, 2009.

[9] J. Xiao and P. Flandrin, "Multitaper time-frequency reassignment for nonstationary spectrum estimation and chirp enhancement," *IEEE Transactions on Signal Processing*, vol. 55, no. 6, pp. 2851–2860, June 2007.

[10] R. Sassi, L. Mainardi, and S. Cerutti, "Amplitude of dominant t-wave alternans assessment on ECGs obtained from a biophysical model." *International Conference of the IEEE Engineering in Medicine and Biology Society*, vol. 2011, pp. 5872–5875, 2011.

[11] A. Van Oosterom and T. Oostendorp, "ECGSIM: An interactive tool for studying the genesis of qrst waveforms," *Heart*, vol. 90, no. 2, pp. 165–168, 2004.

[12] D. Geselowitz, "Description of cardiac sources in anisotropic cardiac muscle: Application of bidomain model," *Journal of Electrocardiology*, vol. 25, no. SUPPL., pp. 65–67, 1992.